

# Multi Objective Horizontal Tail Optimization of a Jet Trainer Aircraft

*Fazil Selcuk Gomec\* Serkan Sagiroglu\*\* Emre Can Unver\*\*\* and Mehmet Zeki Arisoy\*\*\*\**

*\*Aerodynamics Department, Turkish Aerospace*

*Ankara 06980, Turkey*

*\*\*Modelling Department, Turkish Aerospace*

*Ankara 06980, Turkey*

*\*\*\*Flight Mechanics Department, Turkish Aerospace*

*Ankara 06980, Turkey*

## Abstract

Horizontal tail design significantly affects the stability, control and performance parameters of the aircrafts. In this effort, a multi-objective horizontal tail optimization approach is developed for a jet trainer aircraft. The geometric limits and flight conditions of the horizontal tail are defined and a design space is created. To create an aerodynamic database generator in the design space, neural networks are trained with CFD simulations. The optimization algorithm is fed by the neural networks. Pitch stiffness, static margin, take-off rotation, trim drag for the cruise and maximum load conditions are investigated during the optimizations.

## 1. Introduction

Since the first invention of Wright brothers, many aircraft designs have been achieved and produced. Each aircraft is produced for its own specific purpose. Inside the flight envelope, it is imperative that the aircraft carry out the desired maneuvers safely. For this reason, engineers and scientists have interested in flight sciences to investigate how aircrafts behave in the direction of design requirements, interpretations and optimizations.

Flight stability and control is an important subject to be considered through a design phase. These topics should be taken into account from the early stages of the aircraft design process [1]. In a conventional design process horizontal tail surface is sized using statistical data from past aircraft designs [2]. Longitudinal static stability is related to the change in pitching moment coefficient with angle of attack, namely  $C_{m_\alpha}$ . For a conventional aircraft in which the pilot directly linked to the control surfaces - pilot directly controls the aircraft – it should be less than zero.

With the integration of digital control systems, stability level can be decreased to a level where the aircraft becomes neutrally stable or even unstable ( $C_{m_\alpha} > 0$ ). This concept is known as relaxed static stability (RSS). RSS offers lower drag and weight through a reduction in horizontal tail area. Reducing the level of static stability also reduces the trim drag and the tail load required to trim the aircraft. However, it would be unsatisfactory to try to control an unstable aircraft for pilots, because a pilot would have to continuously give inputs to the control surfaces. Therefore, integrating a control system is a must. Incorporating a control law design in a conceptual or preliminary design may not be feasible due to the fact that limited data is available.

Apart from the static stability, dynamic stability plays an important role as well. Aircraft dynamics are conventionally decoupled into longitudinal and lateral-directional motions. [4] Longitudinal dynamics have generally two modes. These are short period and long period (phugoid) stability modes. Damping ratio, natural frequency and the time to double of these modes can be calculated and checked according to Agard-CP-508 [5]. In the short period mode, motion occurs at nearly constant speed but there is a changing in angle of attack like an oscillation. It has complex conjugate roots with a moderate to relatively high damping ratio and relatively high natural frequency and damped frequency. In the phugoid mode, motion occurs at constant angle of attack there is a changing in altitude and speed [6]. Dynamic stability concept is out of concern in this study.

For the longitudinal dynamics of a conventional aircraft, horizontal tail is the main control surface to consider. To assess the horizontal tail performance in terms of control authority, take-off rotation, trim at low dynamic pressure and maximum load factor maneuvers (pull-up, push-down) can be considered [7].

Chen et al. studied on optimizing wing-body-tail configurations for Common Research Model (CRM), which is a transonic transport aircraft model. As fitness function, they selected to minimize trim drag by simultaneous RANS-flow solver. They employed a SQP gradient-based method combined with an adjoint solver due to the large number of design variables [8]. Wang et al. proposed a surrogate model based optimization using a hybrid genetic algorithm. It can eliminate the disadvantages of computing local minima for gradient-based optimizations [9]. Mastroddi and Gemma focused on a multi-objective analysis in weight, aerodynamics and performance issues with high fidelity tools. They also employed SQP gradient-based method [10]. Andrews and Perez optimized a box-wing concept for regional jets that can correspond the horizontal tail effects. They defined a mission profile representing take-off, climb and cruise conditions to minimize the fuel consumption as the optimization objective [11]. Schmitt et al. designed and horizontal tail airfoil to extent the laminar region that enables decrease the drag at transonic cruise conditions [12].

In this study, the main goal is to optimize an all movable horizontal tail for a jet trainer which results in a relaxed longitudinal stability. It enables much more maneuverability and it is one of the requirements for the modern fighter and jet trainer aircrafts. A multi objective optimization approach is utilized in the aspects of static margin, derivative of pitch moment with respect to the angle of attack ( $C_{m_\alpha}$ ), take-off rotation, trim and maneuver drags. To achieve the objectives aspect ratio, taper ratio, leading edge sweep, horizontal tail planform area and hinge line position on the horizontal tail are selected as the design variables. To eliminate the local minima disadvantage of the gradient based methods, MATLAB®'s genetic algorithm tool is employed with artificial neural networks. A design space is created by Latin hypercube sampling and 3D RANS flow simulations are done at the design space. The outputs of the flow simulations are used in the trainings of artificial neural networks. Then, an aerodynamic database generator is created with these trained networks and implemented into the fitness function with the selected objectives.

## 2. Optimization Model

In the optimization process, the preliminary design of Hurjet is selected as the base aircraft. It is a jet trainer aircraft which is under development. During the optimizations a design space for the horizontal tail geometric parameters is computed by Latin hypercube sampling and the corresponding CFD meshes are created. All cases including the meshes are simulated by a RANS flow solver for the selected flight conditions. To generate the aerodynamic data on the input geometric parameters, artificial neural networks are utilized by NNGA which creates optimized neural networks [13]. It enables the data generation without additional CFD runs. The outputs of the flow solver are used as training data of neural network analyses. The fitness function including the desired objectives is written. The center of gravity updates/translations and weight modifications are achieved in the fitness function. The multi objective genetic algorithm is selected as the optimization method and the fitness function is implemented into this algorithm with its constraints. It converges to the minimum values of the fitness function which are called as the design points.

### 2.1. Geometric Parametrization and Design Space

To satisfy the selected objectives, the horizontal tail of Hurjet should be properly parametrized. The horizontal tail geometry is defined by dihedral angle, aspect ratio, leading edge sweep, taper ratio, tail area and the hinge line position. Airfoil geometries of the root and tip chord are the same for each configuration. Also, the actuator location in the aircraft is kept fixed. The hinge line position indicates the position of the actuator hinge line on the mean aerodynamic chord of the horizontal tail.

By the evaluation of modern fighter and jet trainer aircrafts, the geometric constraints of these parameters are given in Table 1. Since the current horizontal tail geometry is used as the initial geometry, its details are also provided in this table.

Table 1: Geometric constraints of the optimizations

Parameter	Lower Limit	Upper Limit	Initial (Base)
Dihedral (°)	-10	0	0
Aspect Ratio	2.45	4.2	3.1
Leading Edge Sweep (°)	30	50	36
Taper Ratio	0.10	0.40	0.25
Area (m <sup>2</sup> )	7.0	12.0	9.0
Hinge Line Position*	0.30	0.65	0.45

(\* ) Hinge location is defined with respect to the mean aerodynamic chord of the horizontal tail

To create the artificial neural networks with minimum error, the geometric parameters should be properly represented in the design space. Therefore, 130 different configurations between the geometric constraints are selected by Latin hypercube sampling which is a design of experiment technique. The generated design spaces are shown in Figure 1. To clarify the changes all parameters are shown with respect to the dihedral.

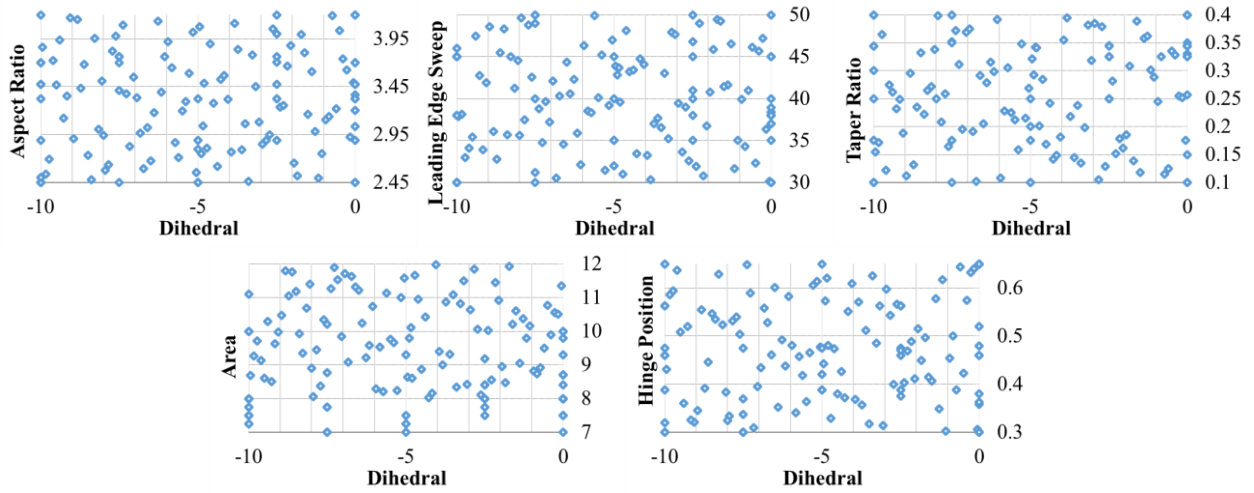


Figure 1: Overview of the design space

It is noted that the area parameter is updated after a few runs. Therefore, the lower limit of the area is decreased to 7 m<sup>2</sup> by stratified Latin hypercube method as seen in Figure 1.

## 2.2. Flow Simulations

As mentioned in the previous section, a design space is formed by 130 different horizontal tail geometries which covers all related parameters. The design space and the flow simulations at each member are used to train the artificial neural networks which are used as the aerodynamic database generator. To calculate all desired objectives, the flight conditions given in Table 2 are simulated by a RANS flow solver.

Table 2: Flight conditions for RANS CFD simulations

<b>Mach</b>	0.2, 0.6, 0.7, 0.8
<b>Angle of Attack</b>	-2°, 0°, 2°, 4°, 7°, 10°
<b>Side Slip Angle</b>	0°
<b>Altitude</b>	Sea Level
<b>Horizontal Tail Deflection</b>	0°, +20°, -20°

It should be noted that horizontal tail deflections of +20° and -20° are only simulated for 0° of angle of attack. The delta values of each Mach regime is added to the clean configuration of the simulations.

Each horizontal tail geometry in the design space and its corresponding mesh and case files are created by Pointwise® scripting. Sample geometries and meshes from the design space are given in Figure 2.

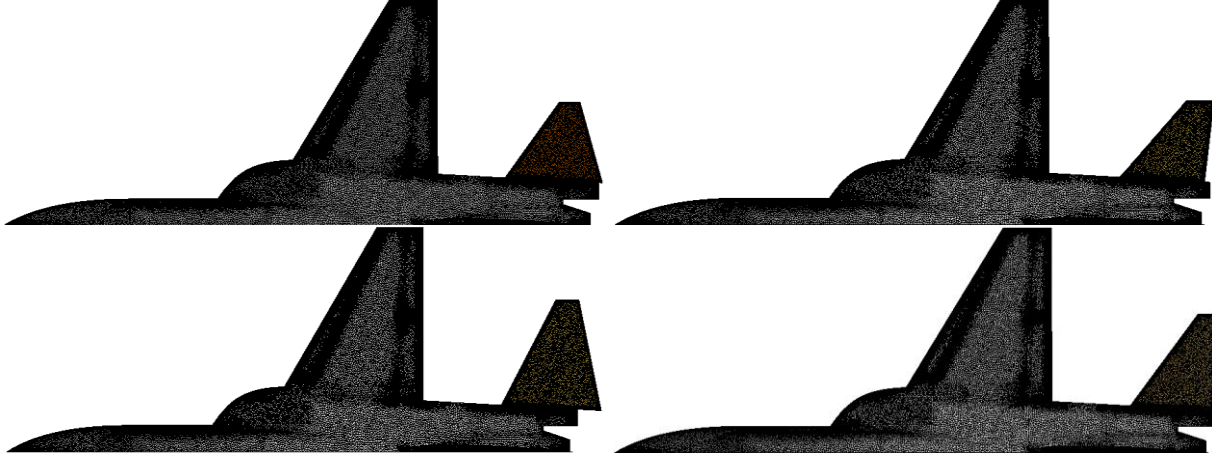


Figure 2: Sample geometries and mesh modifications of the generic model

To simulate all flight conditions for the selected geometries, Ansys®-Fluent is used as RANS flow solver. Spalart-Allmaras turbulence model is selected with energy equation and Sutherland viscosity options. The first order and the second order discretization schemes are assigned with 500 and 3000 iterations. Lift, drag and pitch moment coefficients of each aircraft component are computed and the results are used to train the neural networks. In summary, 40 different flight conditions of 130 geometries in the design space are run. In total, 5200 CFD runs have been successively completed in this study.

### 2.3. Aerodynamic Database Generator

3D RANS flow solvers provide accurate results for the high angle of attack or transonic flight conditions. However, the analyses are time consuming for these flow solvers. Faults or updates in the objectives may result in significant delays in project schedules. Instead of simultaneous geometry updates and CFD runs during the optimization process, artificial neural networks are utilized as the aerodynamic database generator. The design space and flight conditions given in Figure 1 and Table 2 are run by the flow solver and their results are used by NNGA to train the neural networks. NNGA is a script that optimizes the neural network parameters of MATLAB®'s related toolbox [13].

The aerodynamic database generator is a function that outputs the force and moment coefficients at all flight conditions with the related geometric inputs. The database of the deflected geometries can also be provided by this function. It includes the neural networks which are trained by NNGA. Each force and moment coefficients have their own neural networks those inputs are geometric parameters. The inputs should be inside the upper and lower limits provided in Table 1. The fitness function calls the aerodynamic database generator for each run. All objectives are computed with the help of the aerodynamic database from this function.

### 2.4. Center of Gravity and Weight Model

The aerodynamic database generator computes the force and moment on the 25% of the mean aerodynamic center (MAC). The mean aerodynamic center is located on the wing. However, the center of gravity (CG) may vary on the aircraft between forward-CG and aft-CG limits. Therefore, the force and moment is translated on the desired center of gravity (CG) position. The pitch moment translations are done by the equation-1.

$$(C_M)_{TARGET} = C_M + (0.25 - CG_{TARGET}) (-C_L \cdot \cos AOA - C_D \cdot \sin AOA) \quad [1]$$

where  $CG_{TARGET}$  represents the target center of gravity position with respect to MAC and  $(C_M)_{TARGET}$  does the pitch moment coefficients on the target center of gravity. Also,  $C_M$ ,  $C_L$  and  $C_D$  indicate the pitch moment, lift and drag force coefficients.

In addition to the force-moment translations, the center of gravity should also be updated with the changes in the horizontal tail geometry. The changes in the horizontal tail weights reflected as the updates in CG. For this purpose, a weight update module is also written and called by the fitness function. The module uses the equations 2 and 3 [14].

$$W_t = 0.0034 \gamma^{0.915} \quad [2]$$

$$\gamma = (W_{TO} N)^{0.813} (S_{HT})^{0.584} (b_{HT}/t_{RHT})^{0.033} (\bar{c}_{wing}/L_t)^{0.28} \quad [3]$$

where N is ultimate load factor,  $W_{TO}$  is the take-off weight,  $S_{HT}$  is the horizontal tail planform area,  $b_{HT}$  is the span of horizontal tail,  $t_{RHT}$  thickness of the horizontal tail at the root section,  $\bar{c}_{wing}$  is the MAC of the aircraft and  $L_t$  is the tail moment arm.

## 2.5. Fitness and Constraint Functions

The main goal of the optimization is to design a horizontal tail that is suitable for control system to artificially stabilize the aircraft while having adequate control authority at various flight conditions. The fitness and constraint functions start with the geometric inputs of the horizontal tail. It involves the aerodynamic database generator, center of gravity and weight update models. The objectives and constraints are defined and computed in these functions.

For the stability, control system requirements can be translated into aerodynamic parameters. To represent the control system requirement, pitch stiffness ( $C_{m\alpha}$ ) and Static Margin (SM) targets are assumed from Ref [5]. Our target is not to exceed 0.4/rad and -10% of SM at the aft-CG while having appropriate control authority for aforementioned maneuvers. The closer pitch stiffness to 0.4/rad enhances the maneuverability of the aircraft. Therefore, it should be achieved by considering the other objectives and constraints.

For the control authority issues, there are couple of conditions at which the adequacy of the horizontal tail should be demonstrated. These conditions include take-off rotation and capability to generate maximum load factors. In our cases, it is expected to generate maximum load factors by larger deflections of the horizontal tail. Then, the trim conditions during the cruise and maximum-G maneuvers should be satisfied with minimum drag penalties. In trim calculations thrust is excluded. So, the trim point at which the horizontal tail deflection balances the pitching moment of other component except thrust, and angle of attack and horizontal tail deflection combination which creates required lift coefficient. Trim calculations are done at an altitude of 7000 ft. The horizontal tail must have enough control power to initiate the rotation during take-off. To initiate the rotation with  $10^\circ/s^2$ , horizontal tail should have a definite pitch moment output for the horizontal tail rotation of  $-15^\circ$  [4]. The required pitching moment is calculated at  $1.2 V_S$  taking into account the nose landing gear extension. Landing gear extension assumed to *result in*  $2^\circ$  angle of attack. The pitch moment is computed by taking landing gear geometrical parameters into account. It should be noted that the pitch moment requirement for the take-off rotation is the combination of the lift and pitch moments of horizontal tail deflections. To provide the desired take-off rotation, the deflected pitch moment coefficient around the landing gear should not be less than 0.165.

The selected optimization objectives and constraints are summarized in Table 3 and Table 4 with their corresponding center of gravity and flight conditions.

Table 3: Optimization objectives

Objective	Center of Gravity	Flight Condition	Target
Pitch stiffness ( $C_{m\alpha}$ )	Aft-CG	0.8 Mach; $0^\circ$ AOA	0.4/rad
Trim Drag	Forward-CG	0.6 Mach, 1g cruise	Minimize
Max G-Maneuver Drag	Forward-CG	0.8 Mach, 9g	Minimize

Table 4: Optimization constraints

Constraint	Center of Gravity	Flight Condition	Target
Static Margin	Aft-CG	0.8 Mach; $0^\circ$ to $10^\circ$ AOA	$>-10\%$
Pitch moment for the take of rotation	Forward-CG	0.2 Mach, $2^\circ$ AOA	$> 0.165$

## 2.6. Optimization Algorithm

Due to the higher number of input variables, the gradient based methods may fail to find the global minimum and the objective weights should be well defined for the single output fitness functions. Although the higher number of iterations are required, the multi-objective genetic algorithm of MATLAB® is employed to minimize the disadvantages of the gradient based methods. The aerodynamic database generator enables much faster responses for the fitness function with the high accuracy level. It eliminates its disadvantages on the iteration number.

The fitness function and its constraints explained in the previous section are the input of the optimization algorithm. Geometric constraints are also given as the upper and lower boundary. Population size is set to 50. Forward migration direction is assigned and selectionTournament option is defined as the selection function. The current horizontal tail geometry of Hurjet is selected as the initial geometry for the optimizations.

## 3. Aerodynamic Database Validations

In this section, the validations of the aerodynamic database generator which is described in the previous section are done. To validate its outputs, 2 different geometry are chosen and their corresponding coefficients from the RANS flow solver are compared. The validation cases are provided in the Table 5. All validations are done at four different Mach number and six different angle of attack values which are described in the previous section.

Table 5: Validation cases for the aerodynamic model

CASE	Dihedral (°)	Aspect Ratio	Leading Edge Sweep (°)	Taper Ratio	Area (m <sup>2</sup> )	Hinge Line Position
VC-1	-5	3.325	40	0.1	7.25	0.3875
VC-2	-2.5	4	41	0.25	8.4	0.47

The results of the validation cases from NNGA and RANS flow solver are shown between Figure 3 and Figure 6.

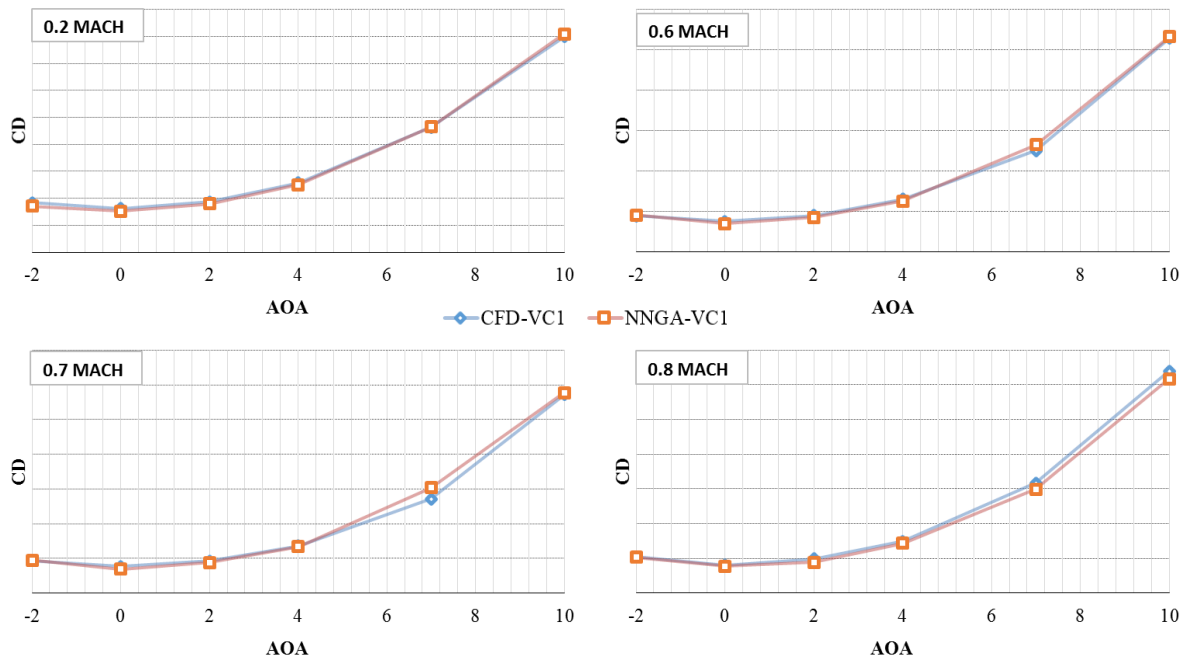


Figure 3: Comparison of drag force coefficients for the validation case VC-1

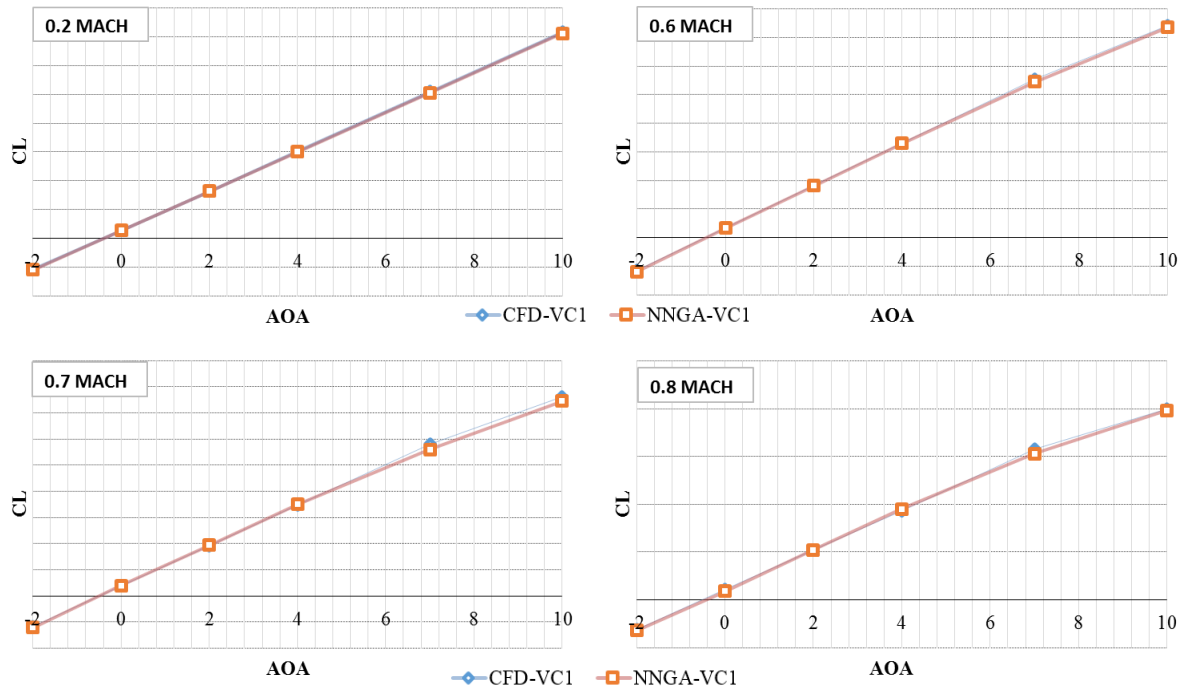


Figure 4: Comparison of lift force coefficients for the validation case VC-1

As seen from Figure 3 and Figure 4, lift and drag components closely match with the outputs of the neural networks. It should be noted that the force and moment coefficients are calculated on the 25% of the mean aerodynamic chord. These forces and moments are translated on the aft and mid center of gravity locations. To minimize the errors in translations, the drag and lift coefficients should be predicted as much as accurate. The comparison of drag and lift coefficients for the validation case-2 are not shown in this section due to the observation of similar results.

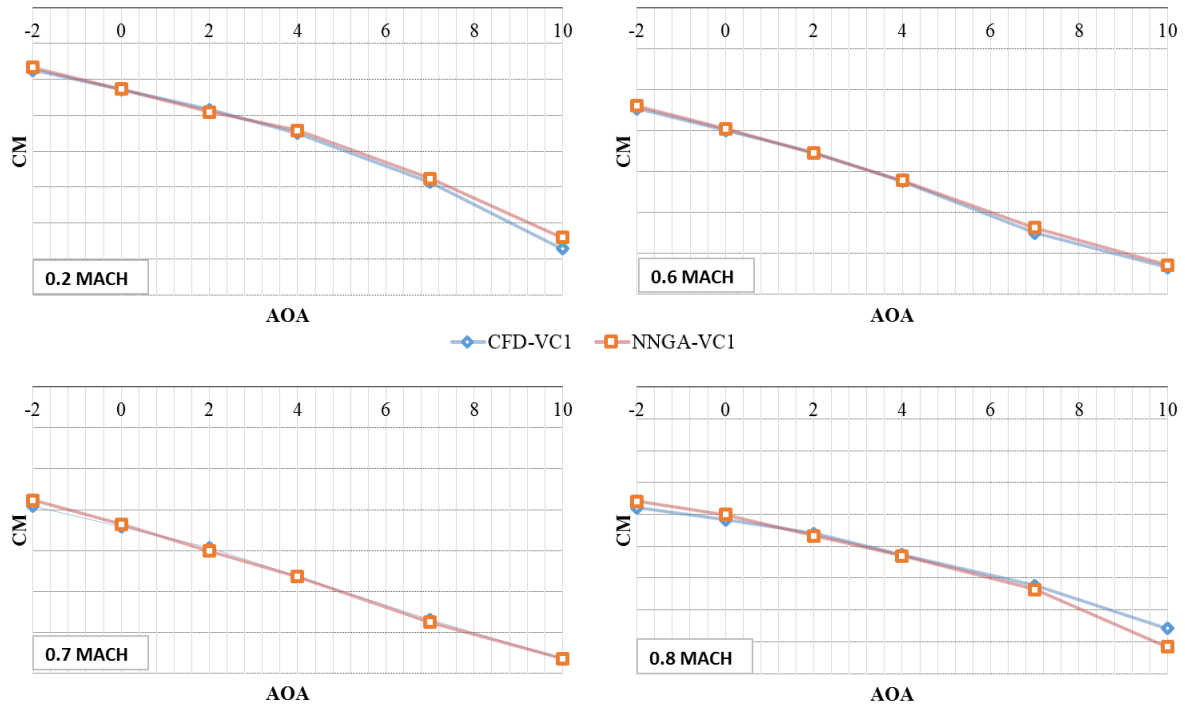


Figure 5: Comparison of pitch coefficients for the validation case VC-1

For both cases, the variations in pitch moment coefficients with respect to angle of attack are provided in Figure 5 and Figure 6. Only the higher angle of attack values at 0.8 Mach may moderately vary from the validation data. If the data generation time and the selected objectives are taken into account, the results of the neural network approach is at the acceptable level to correspond the selected objectives.

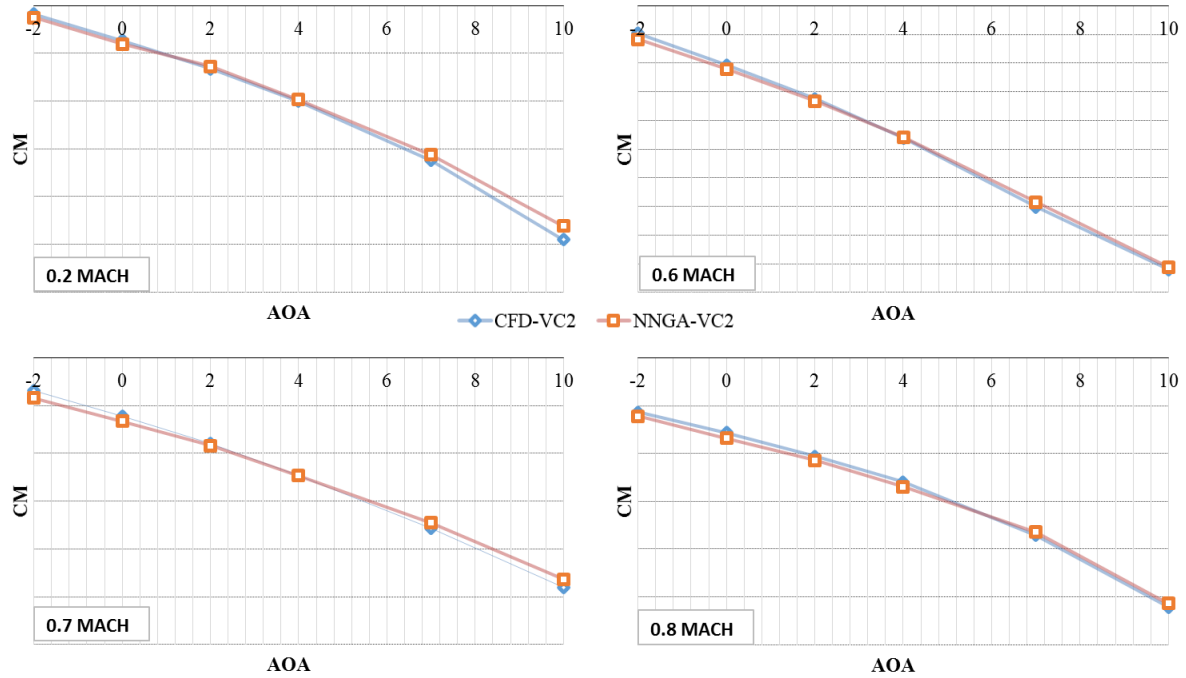


Figure 6: Comparison of pitch coefficients for the validation case VC-2

#### 4. Sensitivity Analyses

In this part of the study, the main target is to show independent effects of each geometric variable on the objectives and constraints. The initial horizontal tail parameters provided in Table 1 are modified to investigate the each parameter. The modifications are shown in Table 6.

Table 6: Sensitivity values for each parameters

Sensitivity ID	Dihedral (°)	Aspect Ratio	Leading Edge Sweep (°)	Taper Ratio	Area (m <sup>2</sup> )	Hinge Line Position
1	-10	2.450	30	0.10	7.00	0.300
2	-9	2.625	32	0.13	7.50	0.335
3	-8	2.800	34	0.16	8.00	0.370
4	-7	2.975	36	0.19	8.50	0.405
5	-6	3.150	38	0.22	9.00	0.440
6	-5	3.325	40	0.25	9.50	0.475
7	-4	3.500	42	0.28	10.00	0.510
8	-3	3.675	44	0.31	10.50	0.545
9	-2	3.850	46	0.34	11.00	0.580
10	-1	4.025	48	0.37	11.50	0.615
11	0	4.200	50	0.40	12.00	0.650

The effects of the parameters are given in Figure 7 with respect to the sensitivity ID's which are provided in Table 6.

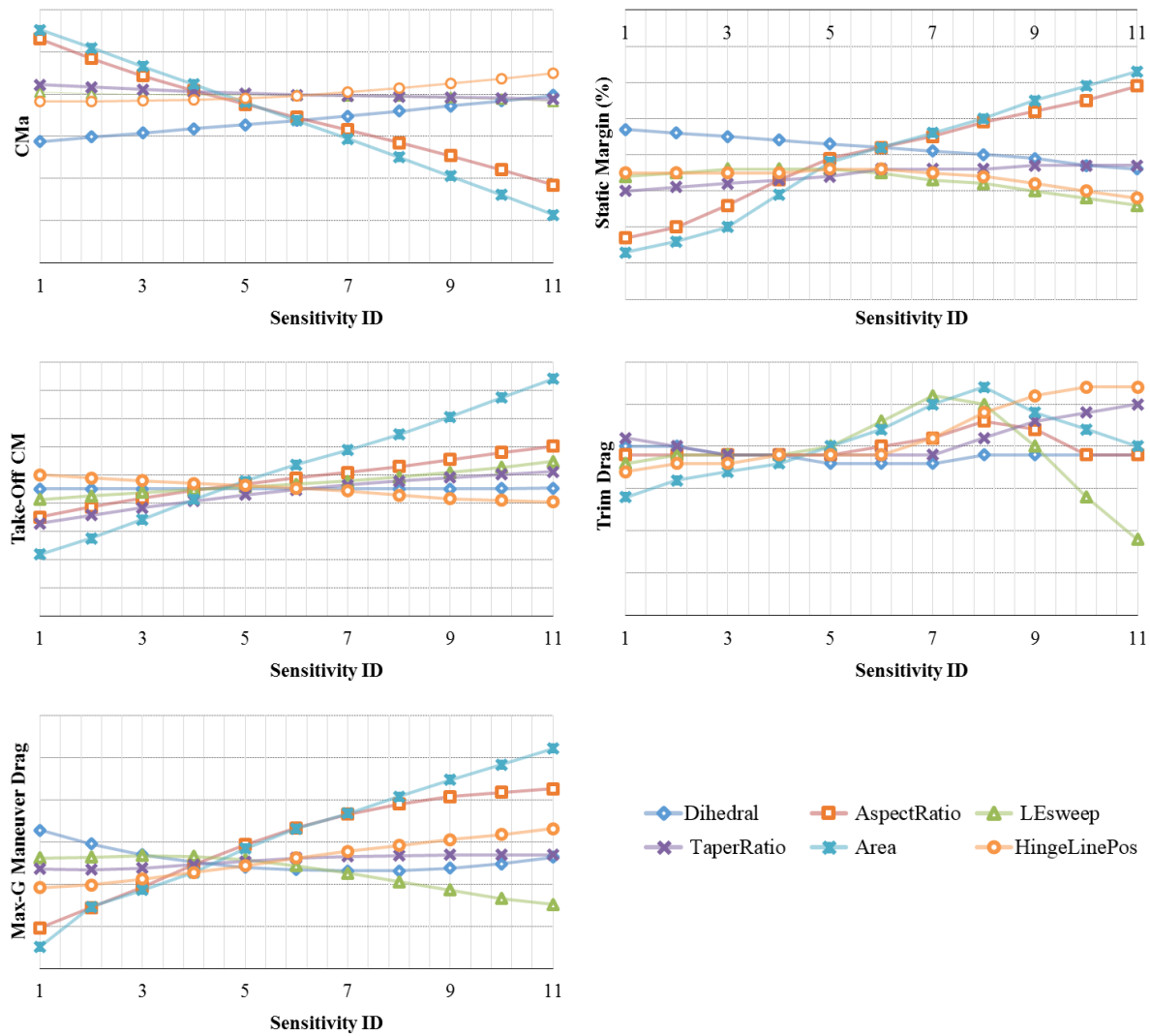


Figure 7: Effects of each design parameter on pitch stiffness (C<sub>Mα</sub>), static margin, take-off pitch moment coefficient (C<sub>M</sub>), trim drag and max-G maneuver drag

As seen from Figure 7, aspect ratio and horizontal tail area significantly influence all objectives and constraints while other parameters are partially effective. Except for dihedral, all parameters can contribute to the take-off pitch moment coefficient. Anhedral angles provide higher static stability than without dihedral cases. On the contrary, negative dihedral angles pose higher drag forces for the max-G maneuver cases. The leading edge sweep, taper ratio and hinge line positions slightly affect the static stability parameters and take-off pitch moment while they can enhance trim drag performance for the cruise and max-G maneuvers. Since all parameters are taken into account for the horizontal tail objectives and constraints, the optimum point of these parameters should be computed for the optimum design point.

## 5. Results

At the end of the optimization process, the design points are calculated with respect to the objectives and constraints. These points are shown in Table 7. For better understanding the progress in design, the initial horizontal tail geometry is also given in this table.

Table 7: The design points after the optimization

Design Points	Initial	1	2	3	4	5
Dihedral	0.0	-5.5	-6.2	-5.9	-3.9	-5.9
Aspect Ratio	3.1	2.48	3.17	2.67	3.23	2.54
Leading Edge Sweep (°)	36.0	43.2	45.6	44.9	40.7	43.0
Taper Ratio	0.25	0.258	0.232	0.316	0.141	0.327
Area (m <sup>2</sup> )	9.0	8.2	7.4	7.6	8.1	9.0
Hinge Line Position	0.45	0.465	0.406	0.318	0.467	0.395
Pitch Stiffness, $C_{m\alpha}$	0.2985	0.3789	0.3143	0.3719	0.2985	0.3022
Trim Drag	0.0259	0.0255	0.0249	0.0252	0.0255	0.0257
Max-G Maneuver Drag	0.2632	0.2515	0.2515	0.2488	0.2589	0.2576
Static Margin	-6.4	-7.7	-7.3	-7.9	-6.2	-6.5
Take-Off $C_m$	0.1905	0.1652	0.1660	0.1701	0.1666	0.2029

The all design points are computed to correspond better characteristics than the initial geometry in the aspects of objectives and the constraints. The design point-1 is obtained for higher pitch stiffness and maneuverability. The second and third design points minimize the trim and max-g maneuver drags. The design points 4 and 5 are determined for better static margin and take-off characteristics while preserving the performances of the initial geometry.

Pitch stiffness parameters of the first and third design points are very close to each other and they are much higher than ones of the initial and other design points. Also, the third design point has the lowest max-g maneuver drag. Also, it satisfies the static margin and take-off pitch moment constraints. Although its trim drag is slightly larger than the second one, the design point-3 is selected as the optimum design point. The initial and optimum horizontal tail geometries are presented in Figure 8.

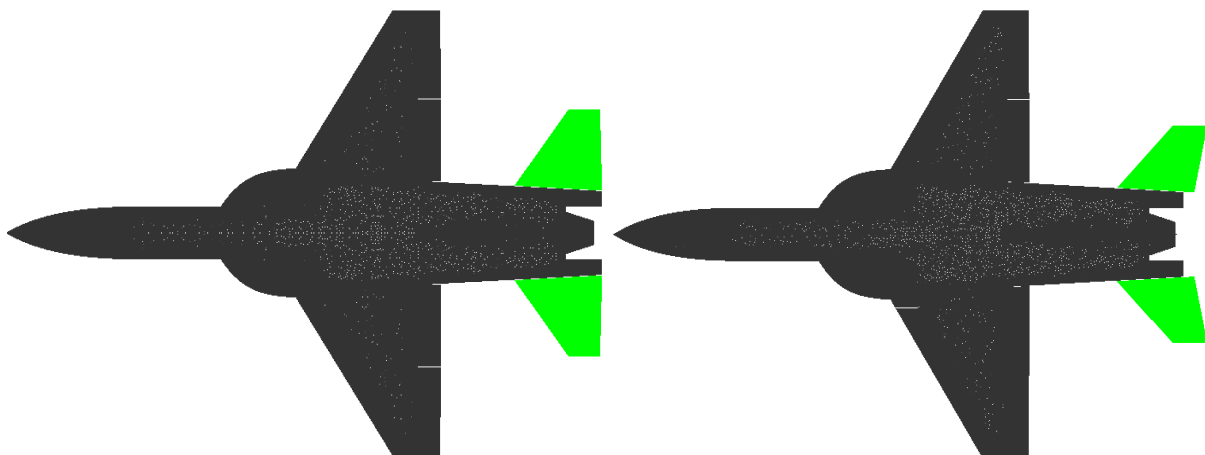


Figure 8: The initial (left) and optimum (right) horizontal tail geometries on Hurjet

## 6. Conclusion

In this study, a multi-objective horizontal tail optimization model is developed for a jet trainer aircraft. Hurjet geometry is evaluated during the optimizations. Dihedral, aspect ratio, leading edge sweep, taper ratio, horizontal tail area and hinge line position are selected as the design variables and a design space is created with 130 different geometries. RANS-CFD simulations are done for these geometries between the flight conditions of 0.2 Mach to 0.8 Mach and 0° to 10° angle of attack. In addition, 20° deflections of these geometries are simulated for 0° angle of attack. The neural networks are trained by the simulations of these geometries and an aerodynamic database generator is created. It enables quick solutions for different horizontal tail geometries without any CFD simulation. The outputs of the aerodynamic database generator are validated by 2 different geometries those data is not used in the network trainings. Equating pitch stiffness to 0.4/rad and minimizing cruise trim and max-g maneuver drag forces are selected as the objectives. Moreover, minimum static margin and take-off rotation constraints are defined as -10% and 0.165 during the optimizations. By updating the initial horizontal tail geometry, the sensitivity of each geometric parameter to these objectives and constraints are investigated. All of the objectives and constraints are highly sensitive to aspect ratio and horizontal tail area. Dihedral is also effective on the pitch stiffness and static margin while the leading edge sweep has significant effects on the cruise trim and max-g maneuver drags. Taper ratio and hinge line position are also significant figures on the cruise trim drag. At the end of the optimizations, an optimum horizontal tail geometry is computed. The pitch stiffness, cruise trim drag and max-g maneuver drag are improved 24.6%, 2.7% and 4.44% as compared with the initial horizontal tail geometry. The most important development is obtained in pitch stiffness which represents the maneuverability of the aircraft.

## References

- [1] J. Welstead and G. Crouse, "Conceptual Design Optimization of an Augmented Stability Aircraft Incorporating Dynamic Response and Actuator Constraints," AIAA, 2014.
- [2] L. Nicolai and G. Carichner, *Fundamentals of Aircraft and Airship Design*, Virginia: AIAA, 2010.
- [3] M. Anderson and W. Mason, "An MDO Approach to Control-Configured-Vehicle Design," in *6th AIAA/NASA/ISSMO Symposium on Multidisciplinary Analysis and Optimization*, Bellevue, 1996.
- [4] J. Roskam, *Airplane Flight Dynamics and Automatic Flight Controls*, Lawrence: DARcorporation, 2001.
- [5] P. Mangold, "Integration of Handling Quality Aspects into the Aerodynamic Design of Modern Unstable Fighters," AGARD-CP-508, Friedrichshafen, 1990.
- [6] T. Yechout, D. Bossert, S. Morris and W. Hallgren, "Aircraft Dynamic Stability," in *Introduction to Aircraft Flight Mechanics*, Reston, American Institute of Aeronautics and Astronautics, Inc, p. 331.
- [7] J. Kay, W. Mason, W. Durham, F. Lutze and A. Benoiel, "Control Authority Issues in Aircraft Conceptual Design: Critical Conditions, Estimation Methodology, Spreadsheet Assessment, Trim and Bibliography," Virginia Polytechnic Institute and State University, Blacksburg, VA, 1993.
- [8] S. Chen, Z. Lyu, G. Kenway and J. Martins, "Aerodynamic Shape Optimization of the Common Research Model Wing-Body-Tail Configuration," in *53rd AIAA Aerospace Science Meeting*, Kissimmee, Florida, 2015.
- [9] K. Wang, Z. Han, W. Song, H. Wang and M. Wu, "Aerodynamic Shape Optimization of Wing-Body-Tail Configuration via Efficient Surrogate-Based Optimization," in *2018 Multidisciplinary Analysis and Optimization Conference*, Atlanta, Georgia, 2018.
- [10] F. Mastroddi and S. Gemma, "Analysis of Pareto frontiers for multidisciplinary design optimization of aircraft," *Aerospace Science and Technology*, vol. 28, pp. 40-55, 2013.
- [11] S. Andrews and R. Perez, "Comparison of box-wing and conventional aircraft mission performance using multidisciplinary analysis and optimization," *Aerospace Science and Technology*, vol. 79, pp. 336-351, 2018.
- [12] V. Schmitt, J. Reneaux and J. Thibert, "Design and Experimental Investigation of a Laminar Horizontal Tail," in *AIAA 8th Applied Aerodynamics Conference*, Portland, OR, 1990.
- [13] F. Gomec and M. Canibek, "Aerodynamic Database Improvement of Aircraft based on Neural Networks and Genetic Algorithms," in *7th European Conference for Aeronautics and Space Sciences (EUCASS)*, Milano, 2017.
- [14] L. Nicolai and G. Carichner, "Weight-Estimation Methods," in *Fundamentals of Aircraft and Airship Design*, AIAA Education Series, 2010, p. 554.